Available online at www.sciencedirect.com
ScienceDirect
Journal of Power Sources 161 (2006) 790–798
JOURNAL OF POWER SOURCES
www.elsevier.com/locate/jpowsour

Processing of carbon composite paper as electrode for fuel cell

R.B. Mathur [a,*], Priyanka H. Maheshwari [a], T.L. Dhami [a], R.K. Sharma [b], C.P. Sharma [b]

[a] *Carbon Technology Unit, National Physical Laboratory, New Delhi 110012, India*
[b] *Soft Polymeric Group, Division of Engineering Materials, National Physical Laboratory, New Delhi 110012, India*

Received 10 March 2006; accepted 29 May 2006
Available online 28 July 2006

Abstract

The porous carbon electrode in a fuel cell not only acts as an electrolyte and a catalyst support, but also allows the diffusion of hydrogen fuel through its fine porosity and serves as a current-carrying conductor. A suitable carbon paper electrode is developed and possesses the characteristics of high porosity, permeability and strength along with low electrical resistivity so that it can be effectively used in proton-exchange membrane and phosphoric acid fuel cells. The electrode is prepared through a combination of two important techniques, viz., paper-making technology by first forming a porous chopped carbon fibre preform, and composite technology using a thermosetting resin matrix. The study reveals an interdependence of one parameter on another and how judicious choice of the processing conditions are necessary to achieve the desired characteristics.

The current–voltage performance of the electrode in a unit fuel cell matches that of a commercially-available material.

Keywords: Carbon fibres; Fuel cell; Porosity; Electrical properties; Paper-making; Composite

1. Introduction

A proton-exchange membrane fuel cell (PEMFC) is an electrochemical cell in which hydrogen is oxidized at the anode and oxygen is reduced at the cathode [1]. Protons released during the oxidation of hydrogen are conducted through the membrane electrolyte while electrons travel through an external circuit to provide an electric current [2]. In addition to the electrolyte, electrodes are also critical for the function of a fuel cell. An effective electrode is one that correctly balances the transport processes required for an operational fuel cell [3].

The electrode must be porous, electronically and ionically conducting, electrochemically active, and have a high surface area [4]. The catalytic activity, physical properties and electrochemical performance must be stable for the duration of the desired cell life. It is rare for a single material to meet all these requirements. Porous conducting carbon paper has been identified as one of the most important components in a fuel cell [5,6]. It not only acts as an electrolyte and catalyst support, but also allows the diffusion of hydrogen fuel through its fine porosity and serves as a current-carrying conductor.

There are a few patents available on the development of such paper and only a few companies are commercially marketing the product. Toray carbon in Japan offers a paper with the following characteristics: (i) porosity > 70%, (ii) density 0.5 g cm^{-3}, (iii) thickness 0.3 mm, (iv) electrical resistivity, 0.005 Ω cm (in-plane), (v) gas permeability 3 mm^2 mm^{-1}. A patent for producing a thin carbon foam electrode suggests freezing polyacrylonitrile (PAN) saturated carbon paper at extremely low temperatures and then applying large pressures for 20–48 h before pyrolyzing the sample [7]. Another patent describes a sol–gel process [8] that takes 4–5 days for completion. Electrodes for fuel cells have also been prepared by forming an exfoliated graphite/phenol resin composite and an exfoliated graphite/glassy carbon composite [9]. These composites were, however, dimensionally less stable because of great carbonization shrinkage and had a low thermal conductivity. Most of the information on electrodes is either protected or does not openly describe control of the many variables and other processing details.

The present study describes the preparation of a porous carbon electrode that possesses high porosity, high electrical conductivity, and sufficient handling strength. It involves a fine dispersion of chopped carbon fibres in an aqueous medium followed by the use of paper-making technology to obtain a highly porous carbon mat. In order to impart strength, the preform

* Corresponding author. Tel.: +91 11 25746290; fax: +91 11 25726938.
E-mail address: rbmathur@mail.nplindia.ernet.in (R.B. Mathur).

0378-7753/$ – see front matter © 2006 Elsevier B.V. All rights reserved.
doi:10.1016/j.jpowsour.2006.05.053

is impregnated with a high char yield resin and carbonized to give an all-carbon composite paper. The properties of the composite paper are found to change with respect to resin content, graphite powder and heat-treatment temperature. The relationship between the process parameters and the product quality is reported for the first time.

2. Experimental

2.1. Materials

A porous carbon fibre preform was prepared with polyacrylonitrile (PAN)-based Toray carbon fibers (T-300) and with pitch-based, high modulus, carbon fibres (Dialed K13A10 from Mitsubishi, Japan). Phenolic resin obtained from 'IVP India Ltd.' was used as a carbonaceous resin for making the composite paper. Colloidal graphite of grade CGAL (methanol) obtained from 'Graphite India Ltd.' was used in some experiments to improve the conductivity and the strength.

The choice of Dialed carbon fibres was based on their high electrical conductivity so as to enhance the overall conductivity of the composite paper. The specific properties of the two selected grades of carbon fibres are listed in Table 1.

2.2. Preparation

2.2.1. Preparation of porous carbon fibre preform

Carbon fibres were chopped into different lengths that ranged from 5 to 20 mm. The chopped fibres were dispersed in an aqueous medium using Triton 100 X as surfactant by vigorous stirring using a high-speed stirrer. Resulting slurry was poured into the container of the specially designed filtration unit shown in Fig. 1. The porous carbon fibre preform of size 10 cm × 10 cm was thus prepared. The choice of chopped fibre length helped to control the pore size in the preform since smaller lengths will result in a smaller pore size.

2.2.2. Moulding of preform with resin

The carbon fibre preform was impregnated with a calculated amount of phenolic resin by means of a hand lay-up process. Calculation of the volume % of the resin for impregnation was made keeping in view the char yield of the neat resin, which was found to be nearly 45%. In the following text, whenever the matrix contents in the composite paper are mentioned these refer to the carbonized resin only, i.e., the carbonized volume of the matrix obtained after heat treatment to 1000 °C. This is termed the 'matrix'. Since the relative volume fractions of fibre and resin affect the properties of the paper, the latter were studied by varying the amounts of the fibre at the expense of the resin. In some cases, graphite was mixed in the resin before impregnating the porous preform. The samples were dried in an oven to remove the solvent and then processed into sheets by a compression-moulding technique. Phenolic resin was cured at 150 °C for 2 h to obtain a green composite paper of thickness ∼0.3 mm. The green sample was characterized in terms of resin uptake, porosity, density, and fibre:resin volume ratio.

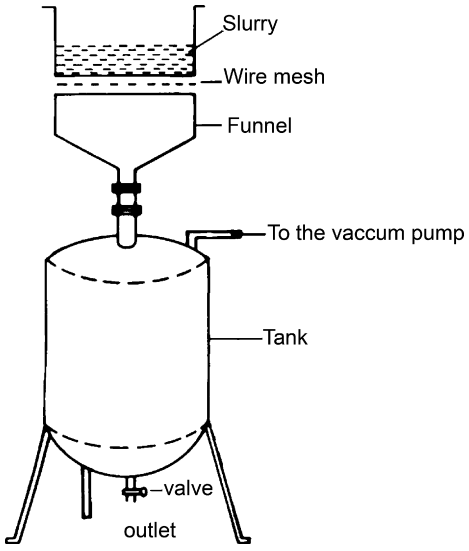

Fig. 1. Schematic diagram of filtration unit for making porous carbon fibre preform.

2.2.3. Carbonization and graphitization of green composite paper

The green samples described above were carbonized to different temperatures (HTT), viz., 1000, 1500, and 1700 °C, in an inert atmosphere at a heating rate of 10 °C h^{-1} up to 600 °C and thereafter at 20 °C h^{-1} up to 1000 °C so that the resin shrinkage was controlled within limits and the porosity and the dimensional stability of the samples was maintained. The carbonized samples were further heat treated up to 2500 °C in a graphitization furnace and then characterized.

2.3. Electrical resistivity analysis

The electrical resistivity (ρ) of the carbonized and graphitized paper was measured using the four-probe technique. A Kiethley 224 programmable current source provided the current. The voltage drop was measured with a Keithley 197 A autoranging microvolt DMM.

The carbon fibre preforms were cut into rectangular strips of size 80 mm (length) and 10 mm (width). The current was

Table 1
Characteristics of carbon fibres for making fibre preforms/mats

Carbon fibre	Tensile strength (MPa)	Y.M. (GPa)	Density (g cm^{-3})	Electrical resistivity (Ω cm)
T-300 (Toray, Japan)	3530	230	1.76	0.0017
Dialed (Mitsubishi, Japan)	2900	790	2.15	0.00047

passed along the length of the strip and the voltage drop was measured across different points separated by unit length. The values reported in the text are an average of about 15 readings over the whole surface of the strip.

2.4. Measurement of flexural strength of composite paper

The flexural strength of the carbon paper samples was measured on an INSTRON machine model - 4411 according to ASTM: D 1184–69: 'Flexural Strength of Adhesive Bonded Laminated Assemblies'. The span length was kept at 10 mm to maintain the span:depth ratio of the test piece at 30:1. The crosshead speed was maintained at 0.5 mm min^{-1}. The properties reported in the text are an average of five readings.

2.5. Fracture behaviour of samples

The stress–strain curves together with the flexural strength of the samples were directly recorded from the software provided with the machine. Fractured surfaces of the individual samples were observed with a, Model Leo S–440, scanning electron microscope.

2.6. Porosity measurements

The porosity of each carbon paper sample was determined by the kerosene density method. The bulk density (B_d) and the kerosene density (K_d) of the sample were measured with a Mettler balance, Model ME - 40290 using Archimedes principle. The porosity was calculated by applying the following formula:

$$\text{porosity} = (1 - B_d/K_d) \times 100\% \quad (1)$$

2.7. Gas permeability measurements

The gas permeability of the samples was determined with a set-up that was designed according to the Indian Standard Method IS: 11056 -1984: 'Determination of Air permeability of Fabrics'. The method is based on the measurement of the rate of flow of air through a given area of fabric by a given pressure drop across the fabric. The permeability was measured in terms of rate of flow of air per cm^2 of the porous paper in $cm^3\ s^{-1}$ by the following formula:

$$R = \frac{r}{A} \quad (2)$$

where R: rate of flow of air per cm^2 of fabric ($cm^3\ s^{-1}$); r: mean rate of flow of air ($cm^3\ s^{-1}$) and A: area of fabric under test (cm^2).

2.8. Optical microscopy

The microstructure of the composite paper was examined with a Zeiss model Axiolab A optical microscope.

3. Results and discussion

3.1. Surface resistivity of carbon fibre perform

3.1.1. Surface resistivity as function of chopped fibre length

Carbon fibre preforms with different chopped fibre lengths were characterized for their surface resistivity. An average of approximately 15–20 readings for each preform sample is reported with a deviation of ±0.2. As shown in Fig. 2, with increase in the chopped fibre length from 0.3 to 1.0 cm, the surface resistivity of the preform decreases from a value of 2.75–1.5 Ω cm^{-2},which is a decrease of almost 50%. Surprisingly, with further increase in the chopped fibre length, the resistivity increases to a value of 3.0 Ω cm^{-2} for preforms made with fibres of 2 cm length. It should be mentioned here that the length of the chopped fibre will also determine the porosity, namely: the smaller the chopped fibre length, the finer will be the size of the pores. An increase in the resistivity of the preform will, however, increase the surface resistivity because of an increase in the contact resistance. It was therefore thought interesting to use a combination of chopped fibre lengths to control the pore size in the preform without sacrificing the conductivity.

A plot of the surface resistivity of the preforms with different combinations of chopped fibre lengths (50% each) is given in Fig. 3. The best results (lowest ρ) are obtained when the preforms

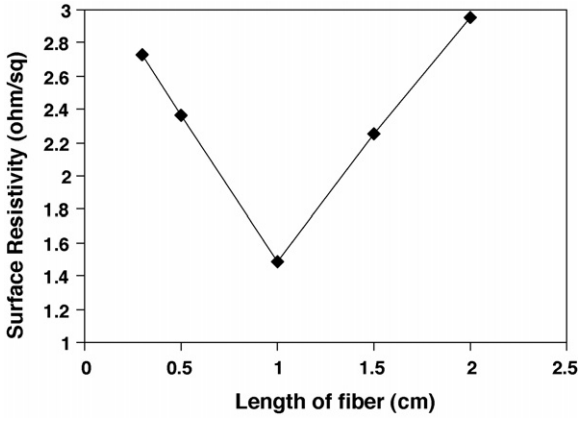

Fig. 2. Variation in surface resistivity of preform with increasing fibre lengths showing minimum resistivity at 1 cm.

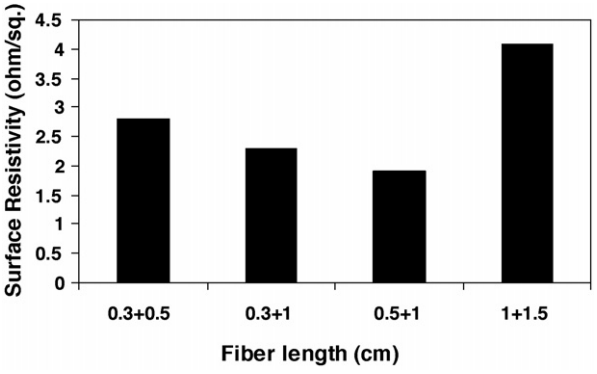

Fig. 3. Variation in surface resistivity of preform with fibre lengths taken in combination.

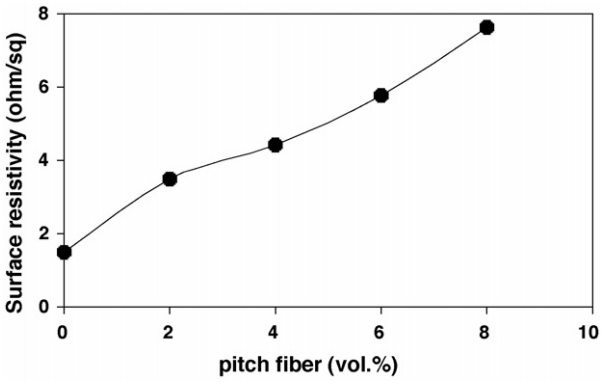

Fig. 4. Increase in surface resistivity of preforms with increasing pitch fibre content.

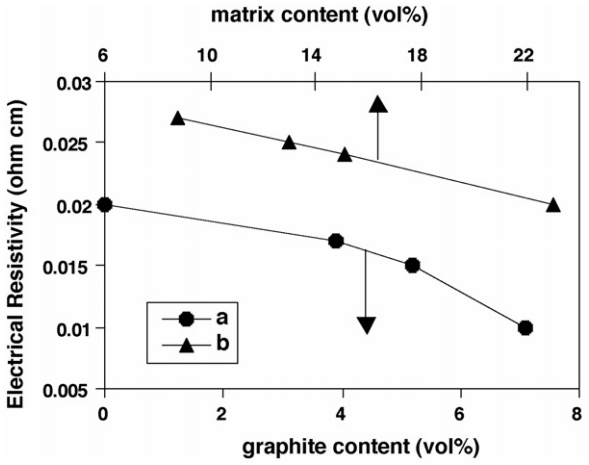

Fig. 5. Variation in electrical resistivity of carbon paper with increasing (a) graphite content and (b) matrix content.

are prepared from a combination of chopped fibre lengths of 1 and 0.5 cm.

To relate the resistivity problem with the theory of percolation [10], a site at which the chopped fibres meet is considered. If an ideally uniform dispersion with all the sites filled is assumed there will be a finite conductivity. For short fibre lengths, there will be an increase in the number of fibres for the same fibre volume. This will increase the number of fibre-to-fibre contacts and lead to an overall high contact resistance. Beyond a certain length, i.e., 1 cm, the increase in resistivity can be interpreted as a lack of formation of proper contacts as the fibre is not dispersed uniformly.

From the above studies, the length of chopped carbon fibre was restricted to 1 cm in all subsequent studies.

3.1.2. Variation of surface resistivity by addition of pitch-based carbon fibres

In order to reduce further the electrical resistivity of the preform, pitch-based Dialed carbon fibres (with electrical conductivity three times that of T-300 carbon fibres) were used to make porous performs. Equal amount of T-300 fibres were replaced with pitch fibres and the total vol.% of the fibres in the preform was kept constant as discussed above. A plot of surface resistivity vs. vol.% of pitch fibre in the paper is presented in Fig. 4. The resistivity increases with increasing vol.% of the pitch fibres. This is contrary to expectation. Optical microscopy and scanning electron micrograph of the preforms showed tiny lengths of fibres that were shorter than those of the original fibres (1 cm), interspersed in the fibrous mat. It is concluded that the highly brittle pitch fibres broke down to very tiny lengths during the vigorous stirring in the aqueous medium. These slip between the fibre-to-fibre contacts of the T-300 carbon fibres and increase the overall contact resistance of the whole preform and thus increase the overall resistivity of the preform.

3.2. Electrical resistivity of composite paper

3.2.1. Effect of matrix contents

Experiments were performed to examine the effect of the matrix content on the electrical resistivity of the composite carbon paper. As shown in Fig. 5(b), the electrical resistivity of the composite paper decreases with increasing matrix content. It is reduced from 0.027 Ω cm for a 8.7 vol.% matrix to 0.02 Ω cm for a 23 vol.% of matrix in the composite paper. The decrease in the resistivity of the samples with increasing matrix content could be the result of graphitization of matrix resin at the fibre|matrix interface. An optical micrograph of a cross-section of the composite paper that contained 23 vol.% carbon matrix is shown in Fig. 6. The columnar type micro-texture of the carbon matrix reveals strong fiber–matrix interactions at the interface. In case of a sample with less matrix (8.7 vol.%) there is no development of anisotropy due to poor fiber–matrix interactions (Fig. 7). Phenolic resin is known to result in hard carbons (a highly crossed-linked structure of crystallites) when pyrolyzed to 1000 °C and above. The electrical conductivity of the pyrolysed resin (carbon matrix) is therefore quite high (∼0.05 Ω cm). In case of composite paper, however, because of the strong fiber–matrix interactions, the fiber|matrix interface tends to graphitize, which leads to decrease in the contact resistance between the filaments [11]. The electrical resistivity therefore decreases and this effect becomes more pronounced when the matrix contents are higher.

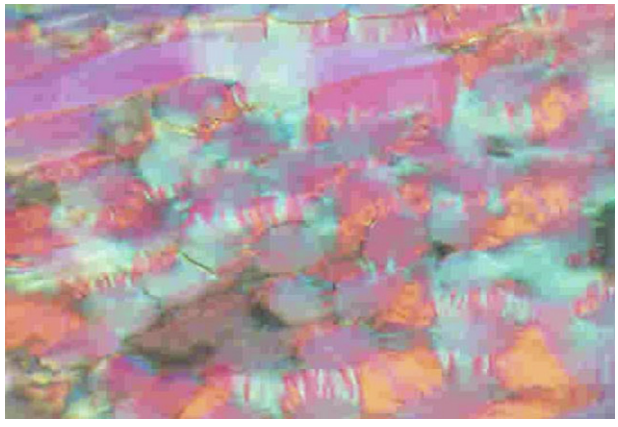

Fig. 6. Optical micrograph of cross-sectional view of carbon sample with 23 vol.% matrix content (×100).

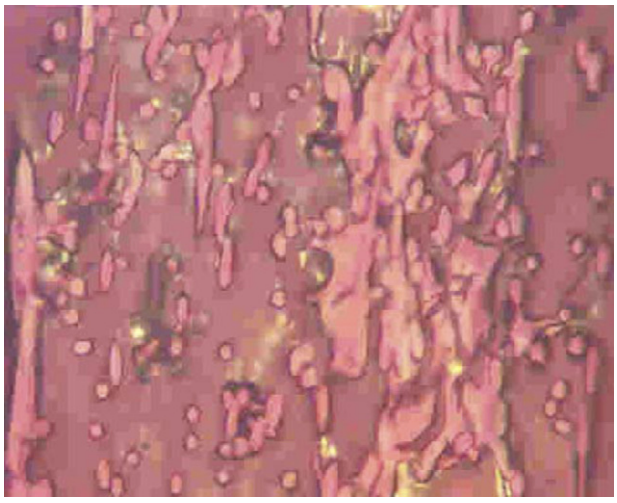

Fig. 7. Optical micrograph of sample with 8.7 vol.% matrix content (×20).

3.2.2. Effect of heat-treatment temperature

Another way to increase the electrical conductivity of carbon paper is through a higher heat-treatment temperature, whereby the structure of the carbon matrix becomes more ordered through stress annealing of the defects at the grain boundaries and increase in the crystallite size. The carbon paper sample with a composition of carbon fibre 11 vol.%, carbon matrix 15% and graphite 4 vol.% was heat treated to 1000 °C and then further subjected to HTT at 1500, 1700 and 2500 °C. The results of resistivity changes in the paper with respect to HTT are plotted in Fig. 8. The resistivity value decreases continuously with increase in HTT. The value is as low as 0.004 Ω cm at 2500 °C. As explained above, the decrease in the resistivity with increasing HTT is due to increase in the degree of graphitization of the matrix at the fiber|matrix interface. Optical micrographs of the samples heat-treated to different temperatures are given in Figs. 9–11. It is evident that the degree of anisotropy, the size of the matrix domains at the fiber|matrix interface and the intensity of the colours, all increase with HTT. The resistivity therefore decreases because of the transformation of the matrix into a highly graphitized structure at 2500 °C.

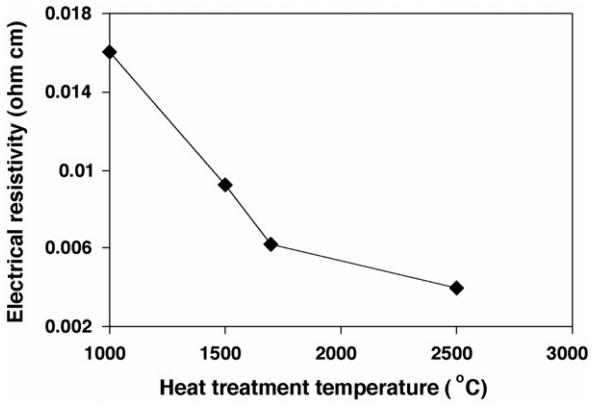

Fig. 8. Variation in electrical resistivity of carbon paper with increasing heat-treatment temperature.

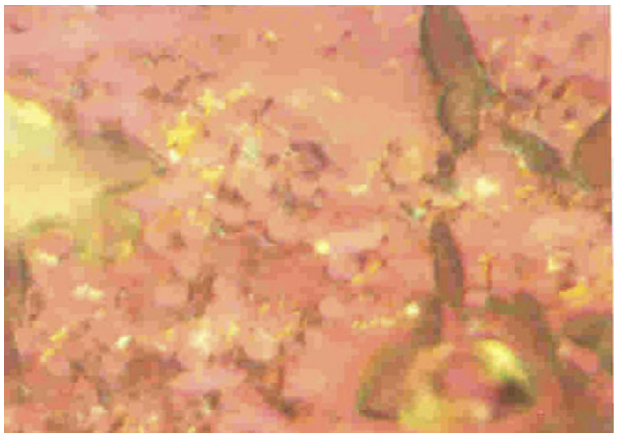

Fig. 9. Optical micrograph of cross-sectional view of sample heat-treated to 1000 °C (×50).

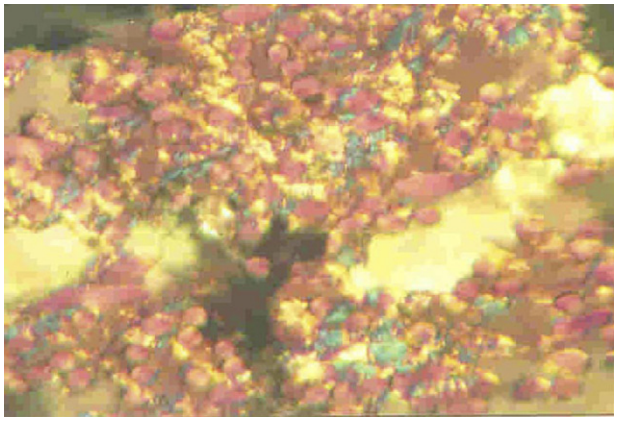

Fig. 10. Optical micrograph of cross-sectional view of sample heat-treated to 1700 °C (×50).

3.2.3. Effect of addition of graphite to the resin

To improve further the electrical resistivity of the paper, a small amount of graphite powder was added to the neat resin before impregnating the preform. The change in the electrical resistivity of the samples with respect to the graphite content in the composite paper is presented in Fig. 5(a).

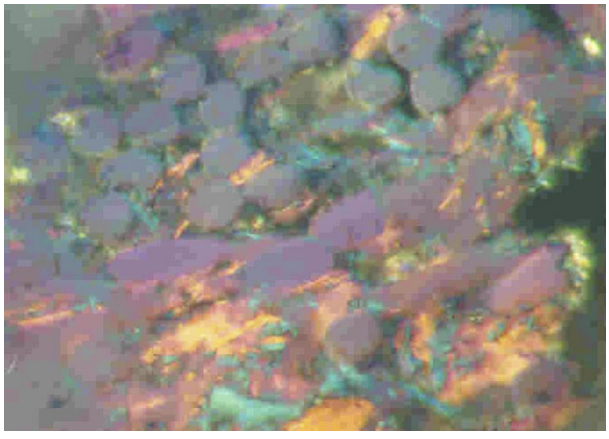

Fig. 11. Optical micrograph of cross-sectional view of sample heat-treated to 2500 °C (×100).

There is a decrease in the resistivity from 0.02 Ω cm for the neat resin to 0.01 Ω cm when 7.1% graphite is added. This behaviour can be attributed to the introduction of a material with higher electrical conductivity (graphite) than that of the carbon fibres.

3.3. Density of composite paper

3.3.1. Variation with matrix content

The variation of the density of the carbonized paper with different volume fractions of the matrix is presented in Fig. 12(b). There is almost a 40% increase in the density when the matrix content increases from 8.7 to 23 vol.%. The result is quite strange given that the density of carbon fibres is higher than that of carbonized resin. Since the overall carbon content in the sample remains unchanged (as discussed above), the rise in density must arise from a decrease in the volume of the sample. The dimensional measurements of the samples reveal that although there is no measurable change in the area of each sample (it remains 10 cm × 10 cm after carbonization), there is a perceptible change in the thickness with increase in the matrix, as shown in Fig. 12(a). The data demonstrate that the thickness of the paper decreases from the desired value of 0.3 mm for matrix contents of <10 vol.% to only 0.22 mm for matrix contents of 22 vol.%. There is 25% shrinkage of the carbon paper sample along the thickness direction during the combined curing and carbonization processes. The high value of shrinkage again reflects strong fiber–matrix interactions due to which the matrix shrinks towards the fibre surface, a consequence generally observed in carbon–carbon composites.

3.3.2. Variation with addition of graphite powder

There is increase in the density of the sample with addition of colloidal graphite from 0.5 g cm^{-3} (without graphite) to 0.69 g cm^{-3} (7.1 vol.% graphite), which is due to the higher density of graphite (2.12 g cm^{-3}) compared with that of T-300 carbon fibre (1.76 g cm^{-3}). The relationship is plotted in Fig. 13(a).

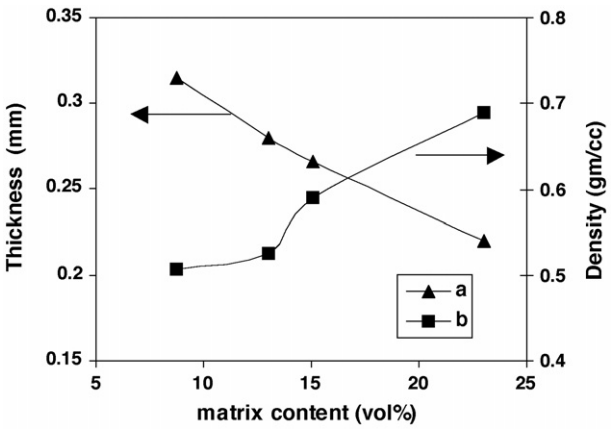

Fig. 12. Variation in (a) thickness and (b) density of carbon paper with increasing matrix content.

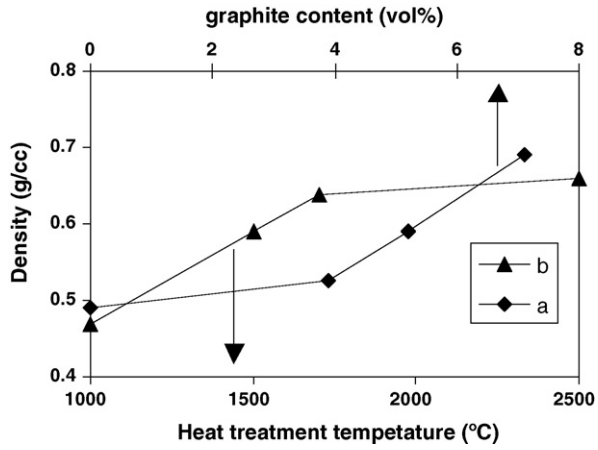

Fig. 13. Variation in density of carbon paper with increasing (a) graphite content and (b) heat-treatment temperature.

3.3.3. Variation with heat-treatment temperature

The variation in the bulk density of the paper with different heat-treatment temperatures is given in Fig. 13(b). The density of the sample increases with HTT due to compaction of the matrix causing overall shrinkage of the material. The density of the paper increases from 0.45 g cm^{-3} for a 1000 °C HTT sample to almost 0.64 g cm^{-3} at 2500 °C. Most of the shrinkage appears to have been completed up to 1700 °C as no change in density is observed beyond this temperature.

3.4. Flexural strength of carbon paper

3.4.1. Variation with matrix contents

The variation in the flexural strength of the carbon paper with matrix content is presented in Fig. 14(b). It is observed that the flexural strength increases with increasing matrix content from 27.4 MPa (8.7 vol.% resin) to 62.35 MPa (23 vol.% resin). The lower value of strength with low matrix contents is a result of high porosity in such samples. This is further confirmed by the optical micrograph of theses samples shown in Fig. 6. The higher strength of the paper with high matrix content is because

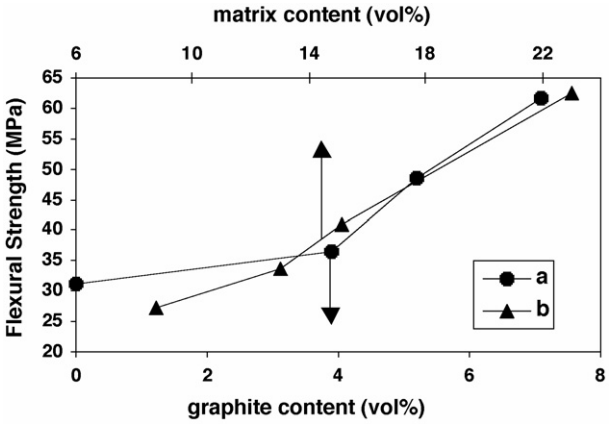

Fig. 14. Variation in flexural strength of carbon paper with increasing (a) graphite and (b) matrix content.

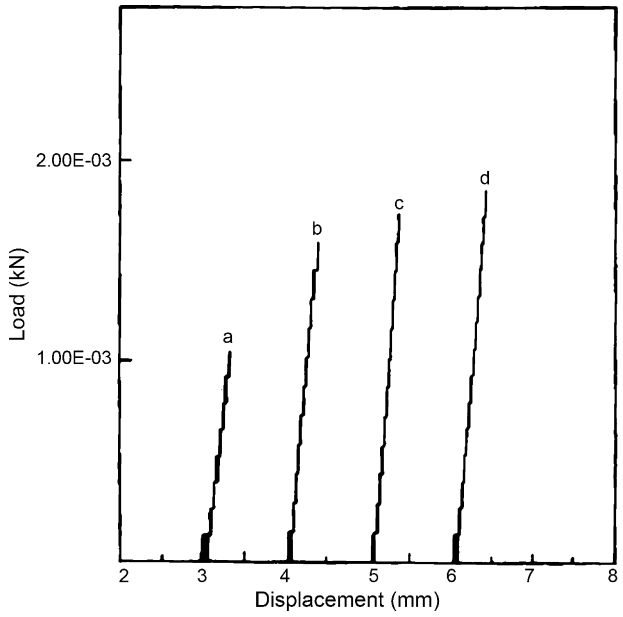

Fig. 15. Fracture behaviour of carbon paper with increasing graphite content. (a) Sample without graphite; (b) with 4 vol.% graphite; (c) with 5.2 vol.% graphite; (d) with 7.1 vol.% graphite.

of sufficient wetting of the complete fibre surface by matrix leading to decreased porosity. This is further confirmed by the strong fibre–matrix interactions shown in Fig. 7.

3.4.2. Variation with graphite content

As explained in Section 3.2.3, carbon composite paper with improved electrical conductivity was produced using graphite additives. These samples were also tested for their mechanical properties. As shown in Fig. 14(a), the strength of the paper increases with increasing graphite content, i.e., from 31 to 62.5 MPa as the graphite content is increased from 0 to 7.1 vol.%. Thus, rise of almost 100% in the flexural strength is achieved. The pores in the paper that can act as crack initiators are blocked by the addition of colloidal graphite, which decreases the porosity and thereby increases the strength of the sample.

3.4.3. Fracture behaviour of composite paper

The fracture behaviour of the composite carbon paper with increasing graphite content is given in Fig. 15. Unlike the fracture behaviour of a true carbon–carbon composite, which is a linear stress–strain brittle fracture [12], the failure behaviour of the paper shows several steps before the ultimate brittle fracture. This suggests multiple fiber–matrix debonding before the final fracture. The fractured surfaces of the samples were observed under scanning electron microscopy. Typical fracture behaviour of the composite paper samples without and with graphite is shown in Figs. 16 and 17, respectively. In the former case, there is considerable fibre pull out that indicates poor fiber–matrix bonding, however with addition of graphite (Fig. 17), the fracture surface is quite smooth. This also explains the higher value of flexural strength of the samples prepared with graphite inclusions in the matrix.

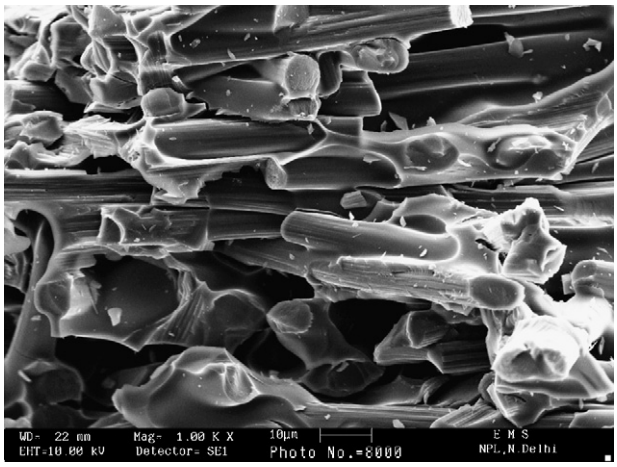

Fig. 16. Scanning electron micrographs of fractured carbon paper surface showing fiber pull-out.

3.4.4. Variation with heat-treatment temperature

The flexural strength of the paper increases with heat-treatment temperature and reaches a maximum of 65 MPa at about 1700 °C. The increase in strength is due to an increase in the fiber–matrix interactions as revealed by optical micrographs of the samples (Figs. 9 and 10). The decrease in strength above 1700 °C (Fig. 18) is normal for carbon–carbon composites prepared with non-graphitized carbon fibres [12]. The strong fiber–matrix interactions lead to graphitization of the matrix carbon at the fiber|matrix interface and the failure of the composite is by shear rather than by a pure tensile process.

3.5. Porosity of paper

3.5.1. Variation with matrix content

The porosity of the composite carbon paper, prepared in different ways as explained above, was measured and compared. As observed in Fig. 19(a), the porosity decreases with an increasing amount of matrix. The porosity decreases from 70.4 to 56.2% as the matrix content increases from 8.76 to

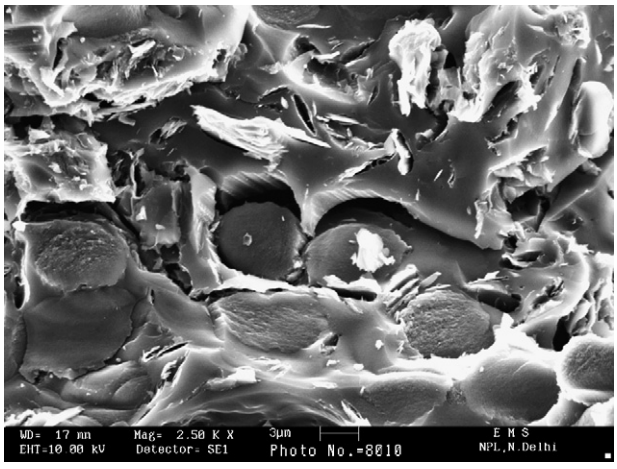

Fig. 17. Scanning electron micrographs of fractured carbon paper surface containing graphite, showing brittle fracture.

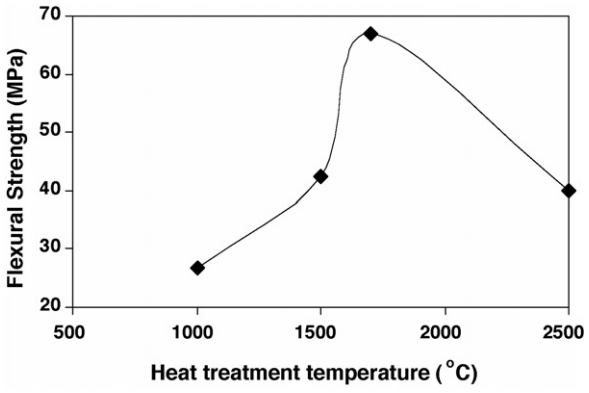

Fig. 18. Variation in flexural strength of carbon paper with increasing heat-treatment temperature.

23 vol.%. As already seen in Section 3.2, there is an overall shrinkage in the paper with increasing matrix content due to the strong fiber–matrix interaction. This causes an overall decrease in the volume of the paper and hence decreases the porosity.

3.5.2. Variation with graphite content

The porosity is also reduced from 70.4 to 61.6% as the graphite content in the sample is increased from 0 to7.1 vol.% (Fig. 19(b)). The decrease is due to the blockage of the pores of the preform by colloidal graphite powder.

3.5.3. Variation with heat-treatment temperature

The porosity of the sample decreases with increasing HTT, namely from 69 to 46.7% from 1000 to 1700 °C, see Fig. 20. Further increase in HTT to 2500 °C leads to a fall in porosity to 32%. It can therefore be concluded that high HTT causes compaction of the overall material that results in a decrease in the porosity.

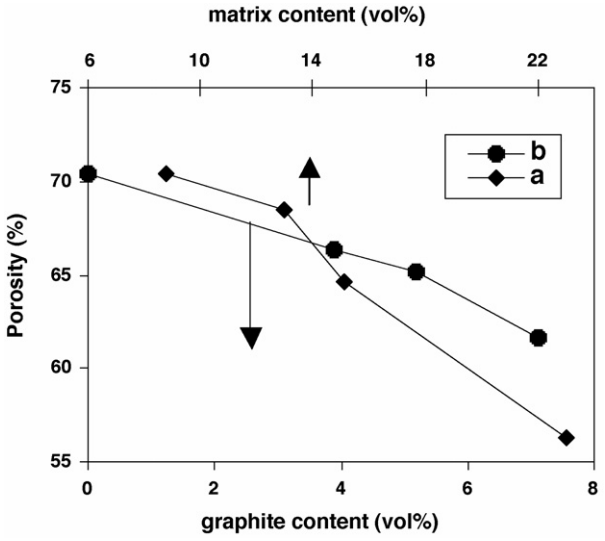

Fig. 19. Variation in porosity of carbon paper with increasing (a) matrix and (b) graphite content.

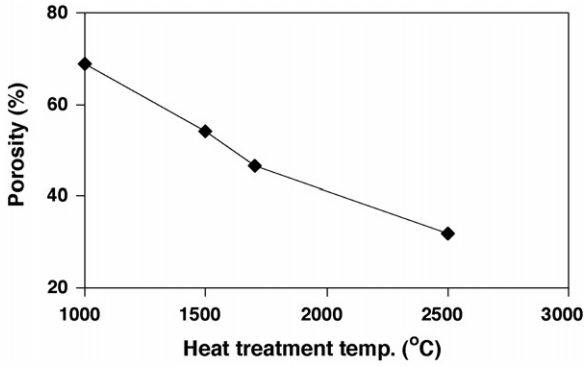

Fig. 20. Variation in porosity of carbon paper with increasing heat-treatment temperature.

3.6. Gas permeability of composite paper

As expected on the basis of the porosity results, the gas permeability of the composite paper decreases with increase in the matrix content as well as in the graphite content. The gas permeability decreases from 3.13 $cm^3\ s^{-1}$ (for 8.7 vol.% matrix) to 2.03 $cm^3\ s^{-1}$ (for 23 vol.% matrix) as shown in Fig. 21(a), which is due to decrease in the porosity of the sample as shown above. Similarly, a gradual fall in gas permeability of the samples is observed with increasing graphite content as shown in Fig. 21(b). The decrease is from 3.8 to 2.4 $cm^3\ s^{-1}$ as the graphite content is increased from 0 to 7.1 vol.%.

3.7. Current–voltage characteristics of composite paper

The current–voltage performance of the composite paper (density = 0.566 g cm^{-3}, $\rho = 0.008\ \Omega$ cm, flexural strength = 42 MPa, porosity ~ 68%, gas permeability = 3.13 $cm^3\ s^{-1}$) was evaluated in a unit cell. The cyclic voltammetry experiments were carried out in 1 N H_2SO_4 and the potential was applied at the rate of 10 mV s^{-1}. The voltammograms of the samples are very similar to that of the commercially available Toray carbon paper, as demonstrated in Fig. 22.

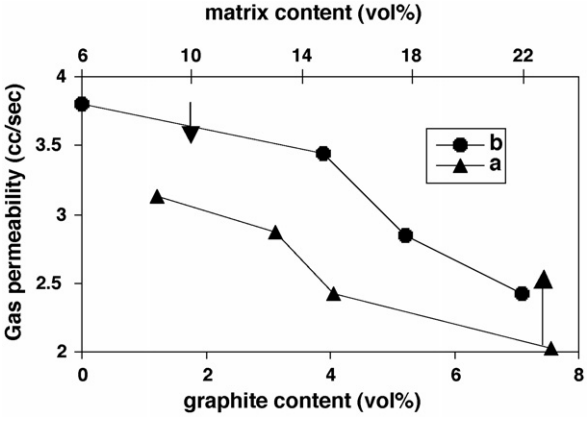

Fig. 21. Variation in gas permeability of carbon paper with increasing amounts of (a) matrix and (b) graphite.

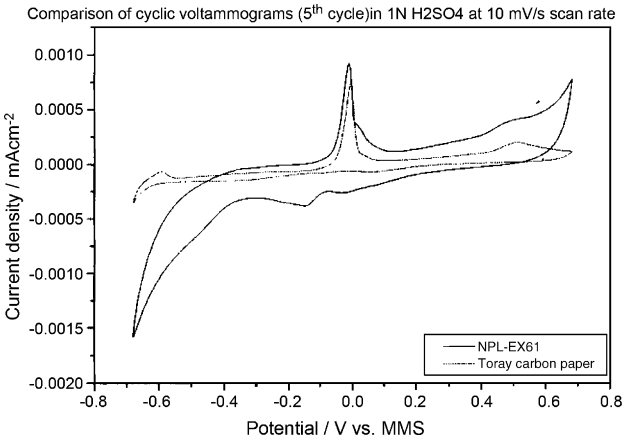

Fig. 22. Comparison of current–voltage performance of carbon paper with commercially available Toray carbon paper.

4. Conclusions

The nature of carbon fibres, chopped fibre lengths, fibre: matrix ratios and the heat-treatment temperature have been found to be important parameters in controlling the characteristics of an all-carbon composite paper that can be effectively used as an electrode for a fuel cell. Cyclic voltammetric studies show that the paper compares well with standard porous carbon paper (commercially available) used in the fuel cells. The dependence of one parameter on the other and their complexities presents challenges in achieving the optimum process conditions.

Acknowledgements

The authors wish to thank Dr. Vikram Kumar, Director, NPL for providing the infrastructure and constant encouragement for the development of the product. Thanks are also due to Dr. Anil K. Gupta, Head, Division of Engineering materials, for fruitful discussions. Assistance from K.N. Sood with the SEM studies is gratefully acknowledged. Evaluation of the cyclic voltammetric performance of the carbon paper by the scientists of Central Electrochemical Research Institute (CSIR), Chennai, is also gratefully acknowledged.

The studies have been carried out under the CSIR NMITLI project ‘Development of Fuel Cells Based on Hydrogen’.

References

[1] M.W. Reed, R.J. Brodd, Carbon 3 (1965) 241–242.
[2] C. Song, Catal. Today 77 (2002) 17–40.
[3] J.M. Odgen, Alternative Fuels and Prospects—Overview, Handbook of Fuel Cells 3: Fuel Cell Technology and Applications, Part 1, Ch. 1, 2003, pp. 11–13.
[4] J. Godat, F. Marechol, J. Power Sources 118 (2003) 411–423.
[5] S. Lister, G. McLean, J. Power Sources 130 (2004) 61–76.
[6] S.M. Haile, Mat. Today (2003) 25–29.
[7] R.W. Pekala, S.T. Mayer, J.L. Kaschmitter, R.L. Morrison, US patent 5932185, 1999.
[8] R. Petricevic, J. Fricke, R. Leuschuer, M. Lipinski, US patent 6503655, 2003.
[9] T. Hirohata, S. Kawakami, US patent 6689295, 2004.
[10] A. Aharony, D. Stauffer, in: Robert A. Meyers (Ed.), Encyclopedia of Physical Science and Technology, vol. 10, percolation, Academic press, 1987, p. 226.
[11] R.B. Mathur, O.P. Bahl, T.L. Dhami, S.K. Chauhan, S.R. Dhakate, B. Rand, Carbon Sci. 5 (2) (2004) 62–67.
[12] O.P. Bahl, T.L. Dhami, Surface energetics interface and mechanical properties of C/C composites, in: K.R. Palmer, D.T. Marx, M.A. Wright (Eds.), Carbon and Carbonaceous Composite Materials—Structure Property Relationship, World Scientific, London, 1996, pp. 255–285.